Recuperated OSL dating of fine-grained quartz in Chinese loess

Wang, X. L.; Lu, Y. C.; Wintle, A. G.

Published in:
Quaternary Geochronology

DOI:
10.1016/j.quageo.2006.05.020

Publication date:
2006

Citation for published version (APA):
Wang, X. L., Lu, Y. C., & Wintle, A. G. (2006). Recuperated OSL dating of fine-grained quartz in Chinese loess. *Quaternary Geochronology*, *1*(2), 89-100. https://doi.org/10.1016/j.quageo.2006.05.020

Available online at www.sciencedirect.com
ScienceDirect
ELSEVIER
Quaternary Geochronology 1 (2006) 89–100
QUATERNARY GEOCHRONOLOGY
www.elsevier.com/locate/quageo

Research paper

Recuperated OSL dating of fine-grained quartz in Chinese loess

X.L. Wang[a], Y.C. Lu[a,b,*], A.G. Wintle[c]

[a]SKLLQG, Institute of Earth Environment, Chinese Academy of Sciences, Xi'An 710075, China
[b]SKLED, Institute of Geology, China Earthquake Administration, Beijing 100029, China
[c]Institute of Geography and Earth Sciences, University of Wales, Aberystwyth SY23 3DB, UK

Received 12 October 2005; accepted 1 May 2006
Available online 24 July 2006

Abstract

The thermally transferred optically stimulated luminescence (OSL) signal from fine-grained quartz extracted from Chinese loess can be separated into two components, the recuperated and the basic transferred OSL signal. The recuperated OSL signal continues to grow with dose, beyond the dose region where the conventionally measured fast component of the OSL signal is close to saturation. A multiple-aliquot, two-part, regenerative-dose protocol, has been developed as a recuperated OSL dating method to extend the application of luminescence dating further back in time. Using the protocol the recuperated OSL signal is separated and used to estimate the equivalent dose for fine-grained quartz in Chinese loess. Ages obtained using equivalent doses determined by the recuperated OSL dating method for 12 samples from the last interglacial–glacial loess–palaeosol sequence are in agreement with multiple aliquot OSL ages and previous stratigraphic information. Ages obtained for four Chinese loess samples from close to the Brunhes/Matuyama (B/M) boundary were also consistent with the expected age of 776 ka. The recuperated OSL dating method, therefore, can go beyond the last interglacial and cover the total Brunhes epoch in Chinese loess.

Keywords: Recuperated OSL dating; Fine-grained quartz; Chinese loess

1. Introduction

Chinese loess provides an outstanding archive of past climatic change (Liu et al., 1985; An et al., 1991). The deposition of dust that makes up the loess is quasi-continuous, occurring in both glacial and interglacial periods. The palaeosols formed in the interglacials are visually recognisable in the field and can be identified by their higher magnetic susceptibility as measured in the laboratory (e.g. Liu et al., 1985; An et al., 1991).

The chronology for these archives has not been established using numerical dating methods. For the youngest part of the deposit, a lithostratigraphy has been established (An and Lu, 1984), identifying loess and soil units. In order to provide a chronology, the boundaries between the soils and loess units within the deposits spanning the last 130 ka have been linked to the marine oxygen isotope records. This allowed the ages for the marine isotope stage (MIS) boundaries calculated by Martinson et al. (1987) to be assigned to the loess sections where this lithostratigraphy can be established.

Luminescence dating has been applied to a small number of loess sections in China. Early thermoluminescence (TL) dating studies (e.g. Lu et al., 1987, 1988, 1999; Forman, 1991) were followed by several dating studies based on infra-red stimulated luminescence (IRSL) (e.g. Musson et al., 1994; Frechen, 1999). Recent comparison of the IRSL signals from Japanese loess deposits have shown them to be underestimated when compared with the optically stimulated luminescence (OSL) measurements made on quartz (Watanuki et al., 2005). Most recently, Lu et al. (accepted) obtained a chronology using a multiple-aliquot OSL procedure on quartz and their ages for the last 130 ka were found to be in broad agreement with the chronology based on the assignment of the MIS boundary ages.

At a greater depth, independent age control is provided by the magnetic polarity reversal of the Brunhes/Matuyama

*Corresponding author. Institute of Earth Environment, Chinese Academy of Sciences, 10 Fenghui S. Road, High-Tech Zone, Xi'An 710075, China. Tel.: +86 29 8832 3864; fax: +86 29 8832 0456.
E-mail address: ych.lu@263.net (Y.C. Lu).

1871-1014/$ - see front matter © 2006 Elsevier Ltd. All rights reserved.
doi:10.1016/j.quageo.2006.05.020

(B/M) boundary, when the Earth's magnetic field changed from reversed to normal polarity (e.g. Heller and Liu, 1982; Liu et al., 1985). The most recent age estimate for the B/M boundary is 775.6±1.9 ka, as obtained from $^{40}Ar/^{39}Ar$ dating of lava flows on the island of Maui (Coe et al., 2004).

In this paper, we present a new OSL dating technique. Our previous studies of the thermally transferred OSL signal (Wang et al., accepted) have suggested that it can be used to extend the range of dating using OSL measurements. In this paper the ages obtained using this signal for samples taken from one site in China will be compared with the ages obtained using a multiple-aliquot OSL procedure for quartz (Lu et al., accepted) and ages inferred from the lithostratigraphic record. Since this data set covers only the last glacial–interglacial cycle (i.e. the last 130 ka), the new technique is also checked using samples from the B/M boundary.

2. Luochuan section—previous luminescence studies

The loess–palaeosol sections at Luochuan (35° 45′N, 109° 25′E) in the centre of the Chinese Loess Plateau have been studied extensively, with their records of climate change in the last 130 ka being of particular interest (e.g. Heller and Liu, 1982; Liu et al., 1985). Previously, two luminescence dating methods have been applied to the loess at Luochuan. Forman (1991) used the TL emission from polymineral fine grains. Lu et al. (1999) obtained 12 TL or IRSL ages for the loess (L_1) above the top of the first major palaeosol (S_1). Neither study was able to obtain reliable luminescence ages over 84 ka. The need for a chronology that extends beyond the last interglacial was highlighted in a recent review of Chinese loess and its role in understanding the evolution of the East Asian monsoon (Huang et al., 2000).

In a more recent study, loess from the Heimugou section at Luochuan has been used to test the sensitivity-corrected multiple-aliquot regenerative-dose (MAR) OSL dating protocol (Lu et al., accepted). Using this protocol on 33 fine-grained quartz samples taken from the upper 13 m of the sedimentary record, down to the base of the last interglacial palaeosol (S_1), good agreement was found with the ages expected from the previously assigned chronology in which lithological units were linked to the climatic changes in the marine oxygen isotope record.

3. Sampling, sample preparation and dose rate determination

For this project, samples were collected from two sections at Luochuan, Heimugou and Potou. Twelve samples identical to some of those used in the OSL study of Lu et al. (accepted) were extracted from the upper 13 m of the Heimugou section (Table A1 in Appendix). These included three samples from the upper part of the Holocene soil (S_0), five samples from the last glacial loess (L_1), and four samples from the first major palaeosol (S_1); the latter is considered to have formed during the last interglacial corresponding to the whole of MIS 5. At the Potou section, the B/M boundary is recorded in the lowest part of the eighth loess unit (L_8) at a depth of 53.4 m (Heller and Liu, 1982; Liu et al., 1985). Two samples were taken at 52.9 and 53.1 m in the eighth loess (L_8) and two samples at 53.8 and 54.3 m in the eighth palaeosol (S_8) (Table A1) in order to provide two samples above, and two samples below, the level of the B/M magnetic reversal.

The preparation of feldspar-free, 4–11 μm diameter, quartz grains from the bulk sediment has been described in detail elsewhere (Wang et al., 2006), together with the equipment used for the OSL measurements. Neutron activation analysis was used to measure the uranium and thorium concentrations of each sample, and the potassium content was determined by flame spectrophotometry. The α efficiency factor was measured for each sample by comparing the OSL signals regenerated by α- and β-irradiation after optical bleaching by a sunlamp (SOL 2) for 3 min, as suggested for TL measurements by Zhou et al. (1995). The dose rate information for all samples is given in Table A1 in Appendix; the values are taken from the previous study (Lu et al., accepted), except those for the B/M boundary.

4. Thermally transferred OSL signals

4.1. Measurement of the thermally transferred OSL (TT-OSL) signal

For optical stimulation with blue light-emitting diodes (LEDs, 475±5 nm), the OSL signal observed in the violet/near-UV part of the spectrum undergoes a rapid decay in the first 5 s of stimulation time. Examples of such decays for naturally irradiated aliquots are shown in Fig. 1(a) for samples IEE210 (MAR OSL age, 1.2±0.2 ka) and IEE223 (MAR OSL age, 50.7±2.6 ka) and in Fig. 1(b) for sample IEE425 (from the B/M boundary). After continuous stimulation for 270 s at 125 °C (Measurement 1 in Fig. 1(a) and Fig. 1(b)), the stimulation was switched off and each aliquot was heated to 260 °C for 10 s. The aliquot was then cooled to 125 °C and the optical stimulation was re-started (Measurement 2 in Fig. 1(c and d)). This resulted in a new, rapidly decaying, OSL signal being superimposed on the slowly decaying component of the main OSL signals in Fig. 1; this is also shown on a linear ordinate scale as a function of time in the insets of Fig. 1(c and d). This TT-OSL signal has been studied in detail by Wang et al. (accepted); this signal contains the OSL signal to be used for dating in the current study.

4.2. Composition of the TT-OSL signal

The TT-OSL signal measured after such a thermal treatment has been known since the earliest studies on the OSL signals of sediments (Huntley et al., 1985; Smith et al., 1986; Aitken and Smith, 1988). TT-OSL signals have been

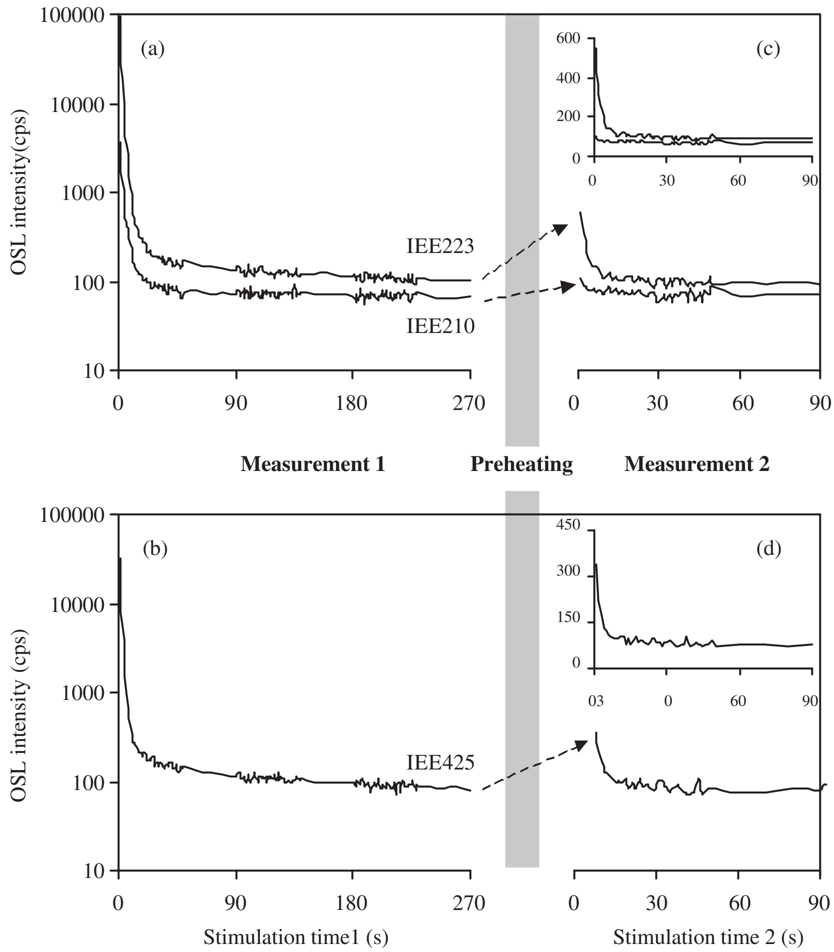

Fig. 1. OSL decay curves of natural fine-grained quartz stimulated by blue LEDs for 270 s (Measurement 1 with Stimulation time (1) for (a) sample IEE210 and sample IEE223, and (b) for sample IEE425 (c and d). After preheating discs at 260 °C for 10 s the TT-OSL signal is measured for 90 s (Measurement 2 with Stimulation time (2), and is also shown on a linear scale as a function of time in the insets. Data are collected in 1 s intervals for 50 s and then in 10 s intervals for the next 40 s for every 90 s measured.

shown to be made up of two types of OSL signals, termed recuperation and basic transfer (Aitken, 1998).

In order for the recuperation effect to occur, electrons will have been transferred into a refuge trap from the OSL traps by light exposure (Aitken and Smith, 1988; Aitken, 1998). In this paper, we define OSL traps as those that give rise to the OSL signal on stimulation at 125 °C. This transfer was occurring whilst other electrons were recombining at luminescence centres that give rise to the OSL signal. Then, thermal transfer of the electrons from the relatively thermally unstable refuge traps into the now empty OSL traps is caused by a subsequent thermal treatment. The next exposure to light gives rise to a new, smaller OSL signal—the recuperated OSL signal. This signal would be expected to be dose-dependent as it is linked to the electrons in the OSL traps prior to the first light exposure, i.e. those that had built up since the exposure to sunlight when the grains had been deposited. Thus the recuperated OSL signal will also be zeroed by light exposure and make it suitable for dating sediments.

In contrast, the basic transferred OSL signal has no potential zeroing mechanism as it is derived from electrons trapped in light-insensitive traps prior to deposition of the grains (Rhodes, 1988; Aitken, 1998); it is thus unsuitable as a dating tool for detrital sediments. In addition, any signal growth with dose would be additional to that which results from electrons that come from the light-insensitive traps with a long lifetime, which are well populated before deposition and may also continue to accumulate electrons after deposition. Electrons in these traps are unaffected by laboratory light exposure, but a small fraction of them are transferred into the OSL traps by a sufficiently high thermal treatment in the laboratory (e.g. 260 °C for 10 s). Therefore the basic transferred OSL contribution should be excluded when dating detrital deposits.

4.3. *Methods of separating the recuperated and basic transfer signals*

The TT-OSL signal can be separated into its component parts by repeatedly preheating (holding at 260 °C for 10 s) and optically stimulating (at 125 °C for 90 s) the same aliquot. This can be seen in Fig. 2(a) for an aliquot of sample IEE425 (from the B/M boundary) where the TT-OSL intensity (obtained by integrating the first 5 s of the signal and subtracting the average signal from the end of the 90 s stimulation) is shown as a function of preheat/OSL cycle. The measured signals (L_{TTOSL}) are corrected for sensitivity change by measuring the OSL response (T_{TTOSL}) to a test dose given after each TT-OSL measurement. The corrected TT-OSL decreases to a constant value of 0.023 ± 0.003 after 6 cycles (Fig. 2(a)). Wang et al. (accepted) have applied the same procedure to a last interglacial sample IEE266 (MAR OSL age, 126 ± 8 ka), and they also found no further reduction in the signal after 6 cycles (Fig. 5(a) of Wang et al., accepted). The constant signal remaining after 6 cycles was interpreted as the basic transfer signal, and the signal that disappears in the first 6 cycles was believed to be the recuperated OSL signal.

It thus seems possible to separate the light-sensitive and dose-dependent recuperated OSL signal from the light-insensitive basic transferred OSL signal, though the above procedure (repeated preheating and stimulation) is not suited to the development of a rapid measurement procedure for dating purposes. Instead, we chose to investigate the use of a short thermal treatment above 260 °C to separate the TT-OSL signal into its constituent parts.

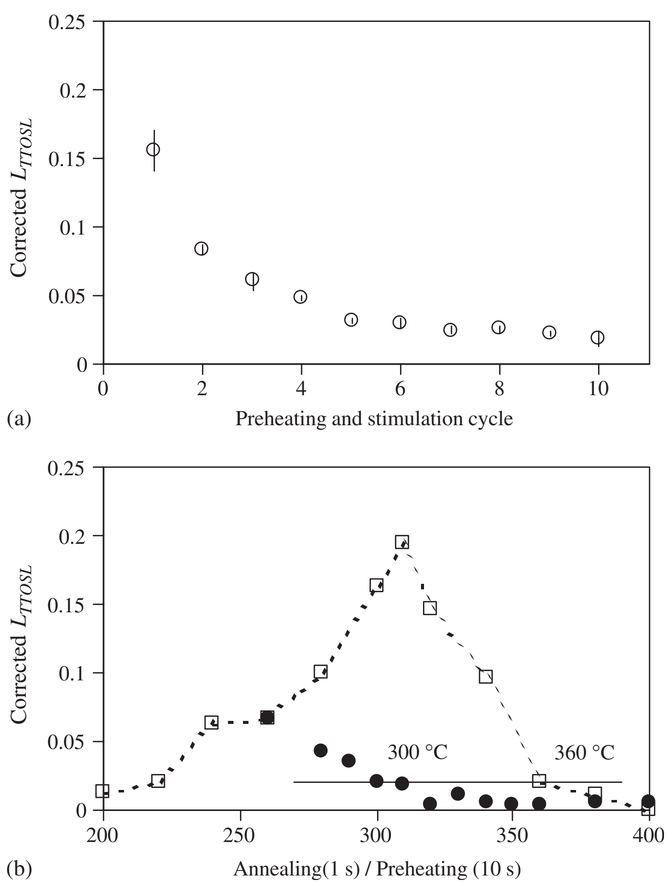

Fig. 2. Sensitivity-corrected thermally transferred OSL signal (L_{TTOSL}/T_{TTOSL}) plotted (a) for repeated cycles of preheat (260 °C for 10 s) and blue stimulation (125 °C for 90 s) as a function of cycle and as a function of (b) annealing (1 s, □) or preheating (10 s, ●) temperature prior to the measurement.

4.4. Effects on the TT-OSL of heating for 1 s

Experiments were carried out on one of the samples from below the B/M boundary (sample IEE425). Twelve naturally irradiated aliquots were first preheated at 260 °C for 10 s to remove electrons from any thermally unstable traps. The aliquots were then exposed to blue light for 270 s at 125 °C to empty the OSL traps and cause electrons to be transferred into the refuge traps. Each aliquot was then heated to, and held for 1 s at, a temperature between 200 and 400 °C (in 20 °C intervals) in order to induce the thermally transferred signals. This short thermal treatment is referred to as "annealing". The resulting TT-OSL intensities (L_{TTOSL}) were measured using blue light stimulation for 90 s at 125 °C. In order to correct for sensitivity change, in much the same way as in the SAR protocol (Murray and Wintle, 2000), the OSL response (T_{TTOSL}) to a test dose of 7.8 Gy was measured, but with a preheat of 20 s at 220 °C being used to remove the electrons from the thermally unstable traps. This correction procedure assumes that the OSL signal from the test dose is appropriate for monitoring the TT-OSL signal. This assumption is currently being tested. Since the TT-OSL and OSL signals are the direct result of electrons being optically ejected from the same traps, it would be expected that the electrons would recombine at the same luminescence centre.

The relationship between the sensitivity-corrected TT-OSL intensity and the annealing temperature is shown in Fig. 2(b) (□). The 10-fold enhancement in the TT-OSL intensity as the annealing temperature is increased from 200 to 320 °C is primarily due to the enhancement of the recuperated OSL signal as more electrons are thermally released from the refuge traps and captured at the OSL traps. As the annealing temperature is increased beyond 320 °C, this effect is overtaken by the thermal ejection of the electrons from the OSL traps. Wang et al. (accepted) showed that the parameters (trap depth and frequency factor) controlling the thermal stability of the OSL traps into which electrons had been thermally transferred by heating for 10 s at 260 °C were identical (within experimental errors) to those for the main OSL signal. Given the thermal stability of the OSL traps, it would thus be expected that no signal would be left after holding for 1 s at 360 or 380 °C. However, a TT-OSL signal is seen (Fig. 2(b)); this is inferred to be the basic transfer signal.

4.5. Selection of preheat conditions for Part 1 of the dating protocol

A preheat of 260 °C for 10 s was selected for Step 1-2 of the new dating protocol (Table 1, Part 1) in order to remove electrons from thermally unstable traps, whilst not touching the electrons in the OSL traps; these would be emptied at temperatures of 320 °C and above (Fig. 2(b)). The same preheat condition was used in Step 1-4 to transfer the electrons from the refuge traps to the OSL

Table 1
Recuperated OSL dating protocol for each disc

Step	Experimental treatment	Result	Note
Part 1. Detection of thermal-transferred OSL signal			
1-1	Dose, D_i	—	For natural samples, $D_i = 0$ Gy
1-2	Preheating at 260 °C for 10 s	—	Removing electrons in unstable TL traps
1-3	Blue stimulation at 125 °C for 270 s	—	Bleaching OSL signals
1-4	Preheating at 260 °C for 10 s	—	Thermally inducing thermal-transferred OSL signals
1-5	Blue stimulation at 125 °C for 90 s	L_{TTOSL}	Detecting thermal-transferred OSL signals
1-6	Give test dose, D_t	—	Monitoring the OSL production in quartz
1-7	Preheating at 220 °C for 20 s	—	Removing electrons in unstable TL traps
1-8	Blue stimulation at 125 °C for 90 s	T_{TTOSL}	Measuring the test dose OSL response
Part 2. Detection of basic-transferred OSL signal			
2-1	Annealing to 300 °C for 10 s	—	Thermally inducing remnant recuperated OSL signals
2-2	Blue stimulation at 125 °C for 90 s	—	Removing remnant recuperated OSL signals
2-3	Preheating at 260 °C for 10 s	—	Thermally inducing basic-transferred OSL signals
2-4	Blue stimulation at 125 °C for 90 s	L_{BTOSL}	Measuring basic-transferred OSL intensity
2-5	Give test dose, D_t	—	Monitoring the OSL production in quartz
2-6	Preheating at 220 °C for 20 s	—	Removing electrons in unstable TL traps
2-7	Blue stimulation at 125 °C for 90 s	T_{BTOSL}	Measuring the test dose OSL response

traps as demonstrated in Fig. 1. This thermal treatment induces a TT-OSL signal equal to that after using a preheat of 280 °C for 1 s (Wang et al., accepted); however, for the dating protocol, thermal treatments of 10 s are preferred to those for 1 s because of better reproducibility.

4.6. Selection of preheat conditions for Part 2 of the dating protocol

Following the measurements used to obtain the TT-OSL signal in Part 1 of the protocol, it is necessary to select an appropriate thermal treatment for Step 2-1. This is the step that would remove any remaining recuperated signal that is not removed by Steps 1-5 to 1-8. To investigate the effects on the TT-OSL signal of heating for 10 s, a second experiment was carried out on sample IEE425. Twelve naturally irradiated discs were treated as in Table 1, but in Step 2-1 the preheat temperature (held for 10 s) was varied, holding at 260 °C, or between 280 and 360 °C in 10 °C steps or in 20 °C steps between 360 and 400 °C. The TT-OSL signals were measured (Step 2-4) and normalised with the OSL response to a test dose (Step 2-7), as shown in Fig. 2(b) (●). As the 10 s preheat temperature in Step 2-1 was increased from 260 to 300 °C, the sensitivity-corrected TT-OSL intensity decreased to the level equivalent to the 1 s anneal data point at 360 °C (Fig. 2(b)); this value of the intensity has been inferred to be the basic transfer signal (Section 4.4). When preheating for 10 s at 320 °C or above, the signal is effectively zero.

From Fig. 2(b), it can be seen that heating for 10 s at 300 °C (or 310 °C) results in a corrected TT-OSL signal of 0.020 (Fig. 2(b)). This is the same signal level that was obtained for the TT-OSL signals for the 1 s anneal at 360 °C, and is thus also inferred to be the basic transfer signal. More importantly, it is the same (within experimental errors) as the level of 0.023 ± 0.003 obtained for repeated cycling (Fig. 2(a)). Thus 300 °C for 10 s was selected as the thermal treatment in Step 2-1 of the dating protocol (Table 1, Part 2) to remove the part of the recuperated OSL signal that survived from Step 1-4 in Table 1. For Step 2-3 the preheat was chosen to be 260 °C for 10 s to transfer the electrons from the refuge traps to the OSL traps (as in Step 1-4).

5. The recuperated OSL dating method

The new dating protocol based on the recuperated OSL signal is given in Table 1, in which the preheat conditions have been selected on the basis of the experimental data of Wang et al. (accepted) and that given in Fig. 2 (Sections 4.5 and 4.6).

First, five or more natural aliquots are measured using the protocol in Table 1 to obtain the intensity of natural L_{TTOSL} and L_{BTOSL}, respectively; the uncorrected L_{ReOSL} intensity would be calculated as

$$L_{ReOSL} = L_{TTOSL} - L_{BTOSL}. \quad (1)$$

For investigation of sensitivity changes during measurements and also for inter-aliquot normalization, two test doses (D_t in Steps 1-6 and 2-5 in Table 1) were interjected after measuring the total thermal-transfer and basic transferred OSL signals. The corrected recuperated intensity, *Corrected* L_{ReOSL}, was then calculated as

$$Corrected\ L_{ReOSL} = [L_{TTOSL}/T_{TTOSL}] - [L_{BTOSL}/T_{BTOSL}]. \quad (2)$$

Each disc was then given a different regenerative dose (D_i) and all the steps in Table 1 were then repeated for each aliquot and the corrected recuperated OSL (L_{ReOSL}) signal for each regeneration dose was also calculated using Eq. (2). The recuperated OSL D_e value for a particular sample was then determined by matching the corrected natural L_{ReOSL} intensity to the dose–response curve constructed using the corrected regenerated L_{ReOSL} intensities. The method is thus a sensitivity-corrected multiple-aliquot regenerative-dose protocol, in which the 15 steps in Table 1 are repeated twice for each aliquot. It is possible that further repetition of these 15 steps could be used as the basis of a single aliquot protocol for recuperated OSL dating. It should be pointed out that the corrected L_{ReOSL} intensities are obtained by taking the difference between two numbers.

6. Dose–response curves for a Holocene sample

The sensitivity-corrected OSL response curve for sample IEE209, constructed using conventional measurements of the OSL signal, was obtained by giving radiation doses to different aliquots in addition to the small environmental dose of about 3 Gy (Fig. 3(a)). The measurement procedure is that developed as the MAR protocol (Lu et al., accepted), with doses up to 3780 Gy being added. The non-linear nature of the dose–response curve obtained for the OSL signals is demonstrated in Fig. 3(a).

A dose–response curve for the L_{ReOSL} signal (obtained using the procedure described in Section 5) is shown for aliquots from the same sample (Fig. 3(b)). For each aliquot a dose was given in addition to the small natural dose and the measurement protocol (Parts 1 and 2 of Table 1) was applied only once to obtain each data point. It can be seen that the recuperated OSL signal continues to grow for doses up to 3780 Gy, the highest dose given here.

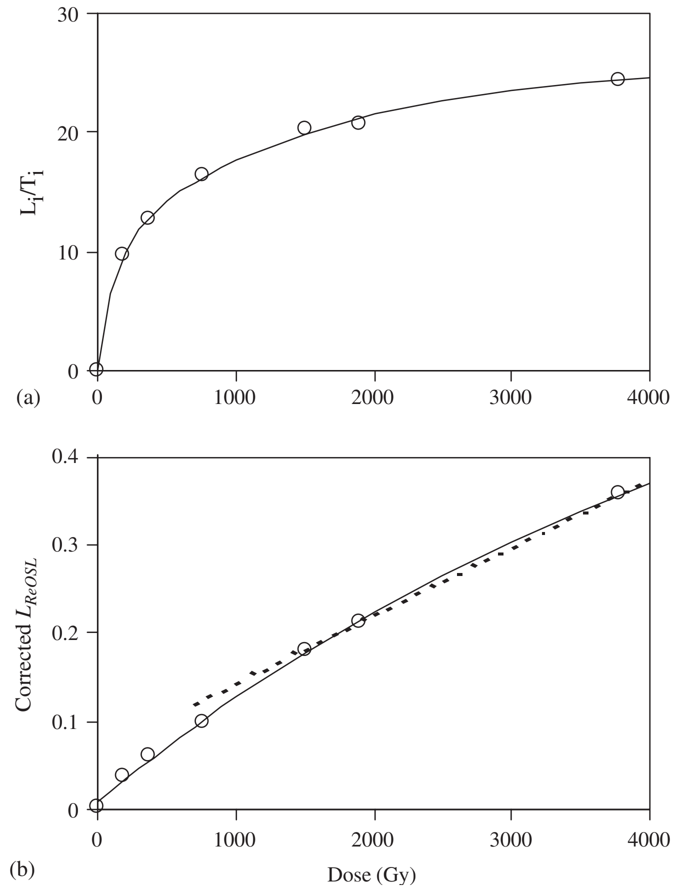

Fig. 3. Sensitivity-corrected (a) OSL (L_i/T_i) and (b) recuperated OSL (L_{ReOSL}) intensity as a function of laboratory dose, with each data point derived from a single aliquot for young sample (IEE209) given radiation doses in addition to the small environmental dose of about 3 Gy. Signal integration time was 5 s. The dashed line in Fig. 3(b) is linear fitting of recuperated OSL intensity against higher doses beyond 1000 Gy, for comparison with the linear trend in Fig. 6(a) for sample IEE424. Both used continuous irradiation at room temperature.

7. Application of the new protocol

The dating protocol of Table 1 was applied to a number of samples. For the Holocene samples and those from the last glacial/interglacial cycle, 6 discs were used to construct the dose–response curves. For the samples from the B/M boundary, 8 discs were used. The sensitivity-corrected values of the natural recuperated OSL signal were projected onto the dose–response curve to obtain the D_e value. The error term in the D_e value is obtained using the deviation of each measured regeneration dose point from the curve that fits the data points and the standard error of the natural recuperated OSL intensity.

7.1. Holocene samples

To test how well the recuperated OSL signal in Chinese loess is zeroed in nature, three Holocene samples (IEE208, 209 and 210 with fine-grained quartz OSL ages obtained using the MAR protocol (Lu et al., accepted)) of 1.1 ± 0.1, 0.8 ± 0.1 and 1.2 ± 0.2 ka, respectively) from the upper part of the Holocene soil (S_0) were dated using the recuperated OSL dating protocol of Table 1. Recuperated OSL dating gave ages of 5.4 ± 0.4, 2.8 ± 0.6 and 2.9 ± 0.7 ka, respectively (Table A1). Thus the recuperated OSL ages are overestimated by a few thousand years. These three samples also demonstrate the large error that is attached to the D_e value obtained for young samples using Eq. (2), as a result of the values of $[L_{TTOSL}/T_{TTOSL}]$ being not much larger than those for $[L_{BTOSL}/T_{BTOSL}]$. In addition, the estimated recuperated signal intensities for these samples (L_{TTOSL} and L_{BTOSL}) were small. For samples IEE209 and IEE210, with values of D_e of 10.0 ± 2.1 and 10.4 ± 2.4 Gy, respectively, the uncertainty is ~22%.

7.2. Samples from the last glacial/interglacial cycle (15–130 ka)

Nine samples, five from the L_1 loess and four from the underlying S_1 soil, were dated using the protocol in Table 1. Fig. 4(a–d) shows the raw data obtained for sample IEE219 taken from the L_1 loess at a depth of 3.5 m. The measured thermally transferred and basic transferred OSL signals are shown as a function of regeneration dose in Fig. 4(e) and the dose–response curve for the recuperated OSL signal calculated from Eq. (2) is given in Fig. 4(f), showing how the D_e value of 122 ± 2.3 Gy was obtained.

This led to a recuperated OSL age of 36 ± 1.5 ka for sample IEE219 (Table A1). For this sample, the D_e value was obtained with very high precision (2%) but for all the older samples in this group, the average precision was 4 ± 1%. This is the result of the small contribution of the basic transferred OSL signal relative to the TTOSL signal seen for all doses over 100 Gy (Fig. 4(e)). The uncertainties in the corrected L_{ReOSL} signal for each regeneration dose point (Fig. 4(f)) are mainly due to the low signal/noise ratio when the basic transferred OSL signal is measured; the signal is of a similar magnitude to the instrumental background. However, it must be mentioned that for sample IEE219, the standard error of natural recuperated OSL intensity is 1.03%, as obtained for the six measured discs. This indicates that there is excellent reproducibility of both the natural and the regenerated data points; thus it is to be expected that it will be possible to recover a D_e value with high precision when using the protocol in Table 1.

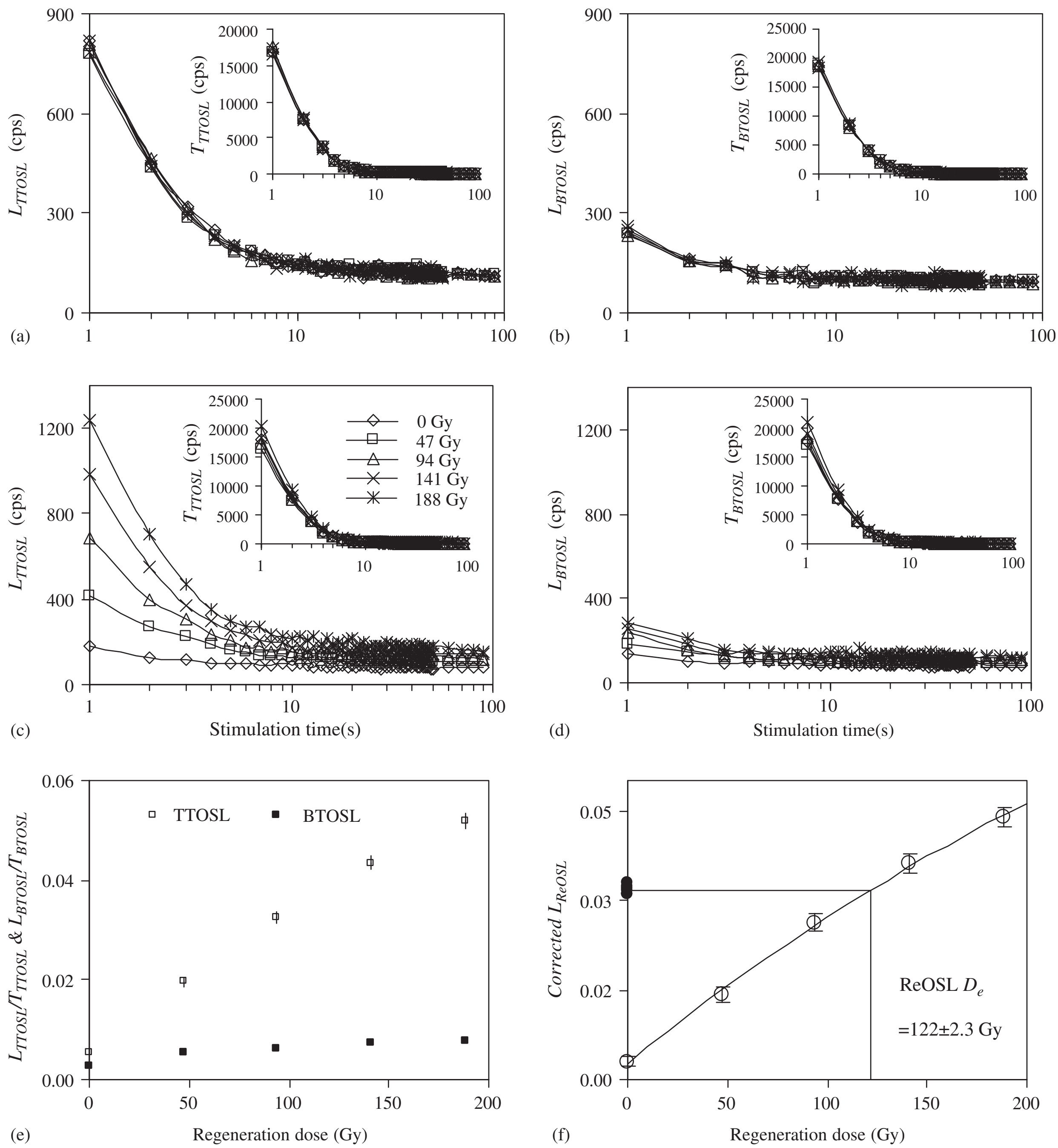

Fig. 4. Recuperated OSL data (collected as stated in caption to Fig. 1) for sample IEE219 (3.5 m below the modern ground surface). Decay curves of (a) natural thermally transferred OSL signal (L_{TTOSL}) and (b) natural basic-transferred OSL signal (L_{BTOSL}); (c) regenerated thermal-transferred OSL and (d) regenerated basic-transferred OSL signals; (e) Dose–response curves for the sensitivity-corrected thermally transferred (□) and basic-transferred (■) OSL intensities and (f) the recuperated OSL signal (obtained using Eq. (2)) and the resulting D_e determination. The insets (in a–d) are the OSL responses to a test dose (7.8 Gy) following their previous measurements.

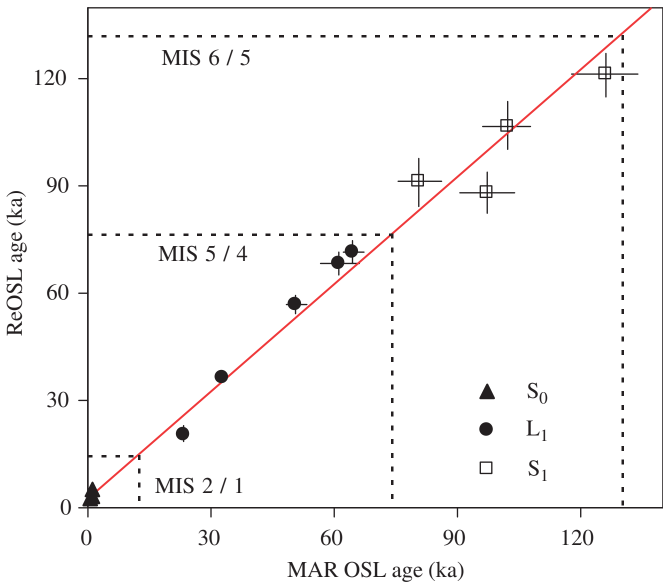

Fig. 5. A comparison of the recuperated OSL and MAR OSL ages for loess and palaeosols of the past 130 ka at Heimugou section, Luochuan. The 1:1 line is given and the Marine Isotope Stage (MIS) boundaries are shown.

All recuperated OSL ages from the last 15–130 ka are given in Table A1. In Fig. 5, the recuperated OSL ages are shown as a function of the OSL ages obtained by the sensitivity-corrected MAR protocol (Lu et al., accepted). The two sets of ages can be seen to be in agreement with each other within uncertainties. The recuperated OSL age estimates of five samples from the last glacial loess (L_1) agree with the SPECMAP ages (Martinson et al., 1987) for the transitions MIS 6/5 (129.8 ± 3.1 ka), MIS 5/4 (73.9 ± 2.6 ka) and MIS 2/1 (12.1 ± 3.1 ka). Sample IEE228, with a recuperated OSL age of 72 ± 3.5 ka, was taken immediately above the lithostratigraphic position of the MIS 5/4 transition. Sample IEE266, with a recuperated OSL age of 121 ± 6.1 ka, was taken from just above the base of the palaeosol S_1 that is equivalent to the lithostratigraphic position of the MIS 6/5 transition. This is taken as validation of the use of recuperated OSL dating for age determination of Chinese loess deposited in the past 130 ka.

8. Dose–response curves for a sample from the B/M boundary

8.1. Using continuous laboratory irradiation

Fig. 6(a) shows the L_{ReOSL} dose–response curve regenerated for an older sample (IEE424 from a depth of 53.8 m) that would be obtained in the course of application of the protocol in Table 1. The values of L_{ReOSL} were obtained using Eq. (2). In the construction of the dose response curve, optical bleaching ahead of the regeneration dose in the second cycle of the protocol (Table 1, Part 1, Step 1) would have been achieved during Steps 1-3, 1-5 and 1-8 in Part 1 and Steps 2-2, 2-4 and 2-7 in Part 2 of the protocol

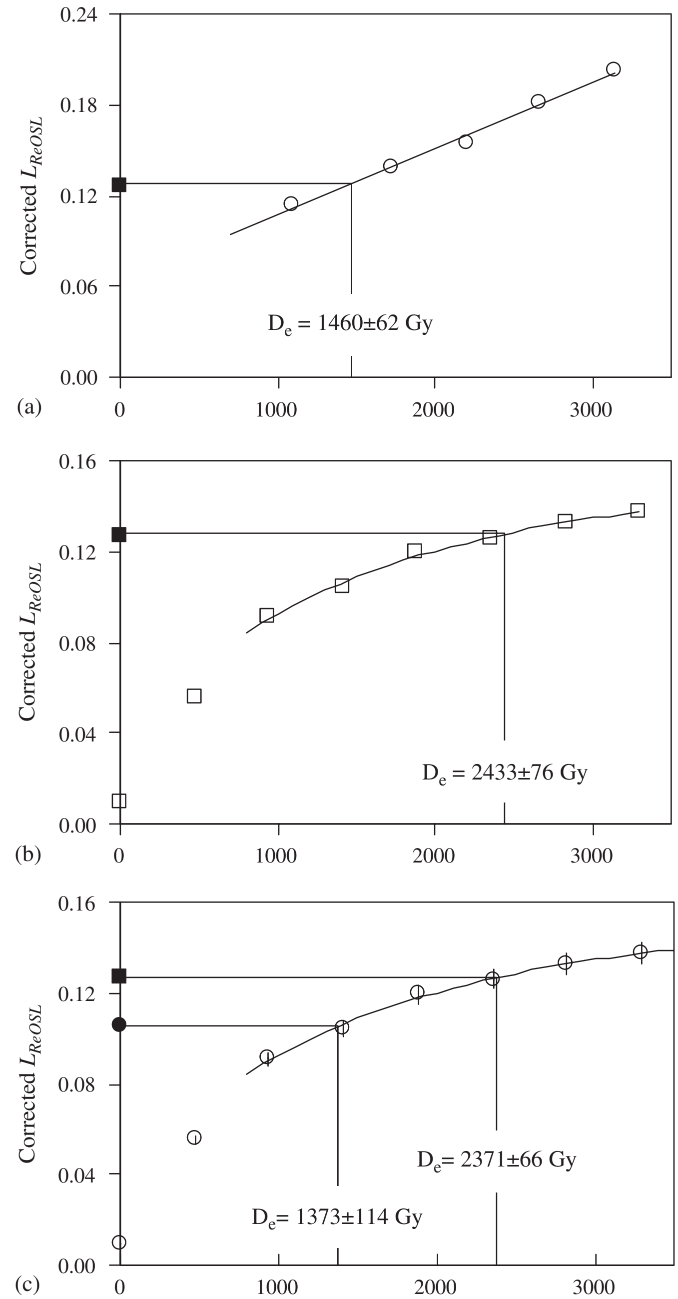

Fig. 6. Corrected recuperated OSL intensity as a function of laboratory dose, for older sample (IEE424) that had been laboratory bleached and given doses with (a) continuous and (b) pulsed irradiation. (c) After recuperated OSL D_e determination illustrated in (b), eight aliquots were separated into two groups, given a known dose of 2355 and 1413 Gy, respectively, and then a dose recovery test was carried out. The 'natural' signal is shown projected onto the dose–response curves giving rise to values of the equivalent dose.

to measure the natural signal. For laboratory doses above 1000 Gy, the L_{ReOSL} appears to grow linearly with dose up to about 3000 Gy, as was found when adding dose to the very young sample IEE209 (Fig. 3(b) dotted line). When the sensitivity-corrected natural L_{ReOSL} intensity is projected onto the dose–response curve (Fig. 6(a)), a D_e value of 1460 Gy is obtained, resulting in an age of only 474 ka. This age is significantly underestimated when compared with the known age for the B/M boundary (776 ka) from which it is taken.

8.2. Using pulsed laboratory irradiation

The severe age underestimation suggests that there is some difference in the recuperated OSL production measured following laboratory irradiation and that measured following irradiation in the natural environment. The most significant difference in irradiation conditions is the rate at which the dose is delivered, with a natural dose rate of about 3 Gy/ka and a laboratory dose rate of 0.157 Gy/s. Valladas and Ferriera (1980) found that by increasing their laboratory γ-dose rate from 0.01 to 10 Gy/s, the TL response of their quartz could be increased by ~10%. Such behaviour has been explained as being due to competition for electrons from relatively thermally unstable traps that are effectively kept empty during natural irradiation (Aitken, 1985). Dose rate dependence has also been suggested as a possible problem for OSL dating of quartz (Chawla et al., 1998; Huntley and Prescott, 2001). A theoretical explanation was proposed by Chen and Leung (2000) using a model with one trap and two recombination centres. Using a similar model with two traps and one recombination centre, Chen and Leung (2001) were able to show a dose-rate dependence of a calculated OSL integral.

It has been suggested that giving irradiation in pulses might provide a better simulation of the trapping conditions in the natural environment (Bailey, 2004). Since the recuperated OSL ages are not underestimated when compared with conventional OSL ages of less than 60 ka in the Heimugou loess section (Fig. 5), the pulsed-irradiation interval was fixed at ~150 Gy; this dose level is reached before onset of acute non-linearity of the quartz OSL dose–response curve. Assuming that the recuperation effect is involved with the 110, 160 and 220 °C TL peaks in quartz (Aitken and Smith, 1988; Spooner et al., 1988; Smith and Rhodes, 1994; Aitken, 1998), the sample disc was heated to 240 °C after each pulsed-irradiation interval. Fig. 6(b) illustrates D_e determination using this approach. Projecting the natural L_{ReOSL} signal onto this dose–response curve (Fig. 6(b)) gives a larger value for the D_e, which will be discussed in the next section.

9. Application of the new protocol to samples from the B/M boundary

Using the protocol in Table 1 for sample IEE424, but giving the laboratory doses in 150 Gy pulses separated by heating to 240 °C, resulted in the dose–response curve for the L_{ReOSL} signal shown in Fig. 6(b) (repeated in Fig. A1 for completeness). The measured data given in Fig. A1(a–d) look very similar to that for the much younger sample (IEE219) shown in Fig. 4. For sample IEE424, the standard error for the natural recuperated OSL intensity is 2.4% for the eight discs measured. For this sample, and the other three samples from the B/M boundary, the precision in the D_e value was 4 ± 1%, similar to that found for the samples from the sediment of the last glacial and interglacial.

The D_e value of 2433 ± 76 Gy combined with a dose rate of 3.08 ± 0.12 Gy/ka (Table A1) resulted in a recuperated OSL age of 790 ± 39 ka for sample IEE424 (0.4 beneath the B/M boundary), an acceptable age for the B/M boundary. The four samples taken close to the B/M boundary gave an average age of 771 ± 15 ka when using recuperated OSL dating, consistent with the recent $^{40}Ar/^{39}Ar$ age of 775.6 ± 1.9 ka recorded in lava flows (Coe et al., 2004).

Further validation of using pulsed irradiation for old samples was obtained by giving known laboratory doses (2355 Gy in 18 pulses and 1413 Gy in 9 pulses) to aliquots previously used for D_e determination of sample IEE424; the measured doses were 2371 ± 114 and 1373 ± 66 Gy, respectively (Fig. 6(c)). The procedure is thus able to recover doses back to 2500 Gy within experimental error; these dose recovery results indicate that it is suitable to use the test dose OSL response to allow for sensitivity changes in the recuperated OSL signal. It should be noted however that these doses were given after the aliquots had already experienced two cycles of the protocol. These results, and the ages for these four samples (Table A1), provide evidence that recuperated OSL dating offers a new method for dating the B/M boundary in Chinese loess. However, the apparent saturation of the corrected L_{ReOSL} signal above 2500 Gy (seen in Fig. 6(b and c)) suggests that this is close to the upper limit of the method.

10. Conclusions

In this paper, we have developed and tested a multiple-aliquot, two-part, regenerative-dose protocol for the recuperated OSL dating of fine-grained quartz in Chinese loess. For samples from the Holocene soil (S_0), the procedure results in overestimation of the ages when compared with a more conventional optical dating method. In addition, because of the need to calculate the difference between the total TT-OSL signal and the basic transferred OSL signal, an error of ~20% in the D_e value is obtained. Thus, this new method appears unsuitable for dating fine grained quartz of Holocene age.

Good agreement of the recuperated OSL ages and conventional OSL ages (derived using the sensitivity-corrected MAR protocol, Lu et al. (accepted)) for samples from the last glacial loess (L_1) and the last interglacial palaeosol (S_1), covering the dating range from 15 to 130 ka, is taken as validation for the new method in the late Quaternary. In addition the ages obtained with the new protocol are in broad agreement with the ages previously assigned for the lithostratigraphic boundaries identified in the Heimugou section at Luochuan.

To obtain correct ages when applying the new protocol to samples from the B/M boundary at the Potou section at Luochuan, it was found necessary to give the laboratory doses in steps of 150 Gy with intervening heating to 240 °C.

The recuperated OSL signals grow to high doses, with significant growth being shown for doses up to 2500 Gy. In order to explain this extended dose response, and using the previous explanation of the recuperation effect, it is necessary to suggest that the production of conventional OSL signals is limited by the number of available luminescence centres. The number of trapped electrons continues to increase with dose to higher dose levels than that implied by the OSL dose–response curves; a portion of these trapped electrons can be sampled by the thermal transfer process. When these are measured, an adequate number of luminescence centres are available. Thus, we propose that recuperated OSL dating offers a new dating method that is able to go beyond the 130 ka limit encountered in many detrital deposits when using conventional OSL protocols. It is now possible to obtain ages for samples with dose rates of ~3 Gy/ka for as far back as 0.8 Ma.

Acknowledgements

We would like to dedicate this paper to the memory of Nicholas Shackleton who, over twenty years ago, encouraged AGW to apply luminescence dating techniques to loess. We thank Prof. An Z.S., Prof. G.A.T. Duller and an anonymous referee for valuable comments on the manuscript. This work was funded by the National Basic Research Program of China (no. 2004CB720200) and the NSFC (no. 40523002).

Appendix

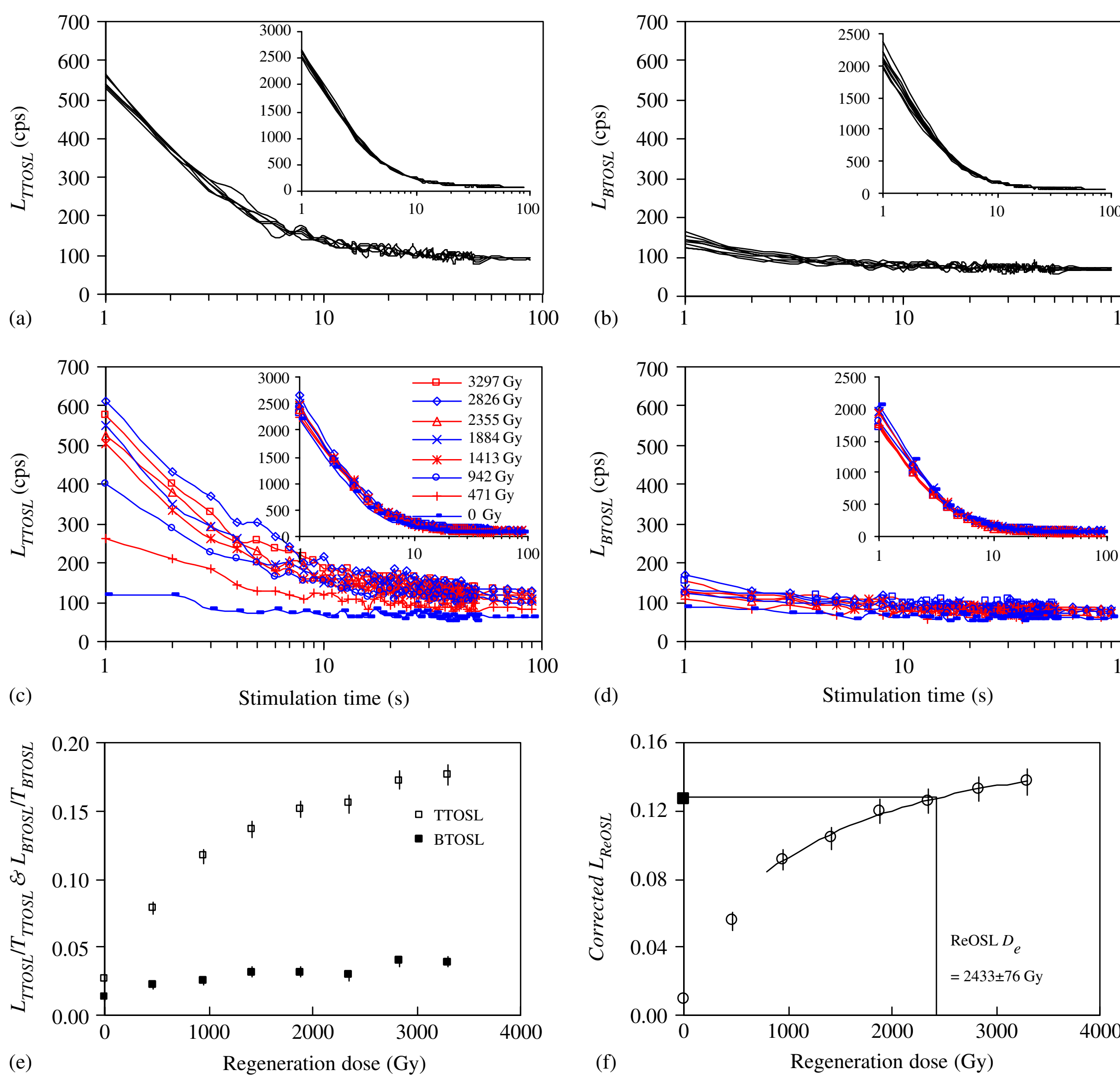

Fig. A1. Recuperated OSL dating of sample IEE424 (0.4 m below the B/M boundary). Decay curves (collected as stated in caption to Fig. 1) of (a) natural thermally transferred and (b) basic-transferred OSL signals; (c) regenerated thermally-transferred and (d) basic-transferred OSL signals. Dose–response curves for (e) sensitivity-corrected thermally transferred (L_{TTOSL}, □) and basic-transferred OSL (L_{BTOSL}, ■) intensity with pulsed-irradiation and (f) The corrected recuperated OSL intensities calculated using Eq. (2) (L_{ReOSL}, ○) obtained using pulsed irradiation and D_e determination. The insets (in a, b, c and d) are the OSL responses to a test dose (7.8 Gy) after the preceding natural and regenerated thermally and basic-transferred OSL measurements.

Table A1
Data for MAR OSL and recuperated OSL age determination

Lab. No	Stratigraphy	Depth (m)	U (ppm)	Th (ppm)	K (%)	Water content (%)	Alpha coefficient	Dose rate (Gy/ka)	D_e (Gy)		Age (ka)	
									MAR OSL	Recuperated OSL	MAR OSL	Recuperated OSL
IEE208	S_0	0.1	2.19±0.08	11.50±0.25	1.86	15±2	0.040	3.48±0.11	3.6±0.2	18.7±1.2	1.0±0.1	5.4±0.4
IEE209	S_0	0.3	2.34±0.09	12.20±0.27	1.90	15±2	0.039	3.60±0.12	3.0±0.4	10±2.1	0.8±0.1	2.8±0.6
IEE210	S_0	0.5	2.46±0.10	13.10±0.29	1.91	18±2	0.039	3.57±0.12	4.3±0.6	10.4±2.4	1.2±0.2	2.9±0.7
IEE215	L_1	2.0	2.39±0.10	11.60±0.26	1.69	15±2	0.048	3.44±0.12	79.8±2.4	71.4±7.2	23.2±1.1	21±2.2
IEE219	L_1	3.5	2.31±0.09	12.20±0.27	2.03	20±2	0.035	3.35±0.12	110±1.5	122±2.3	32.8±1.2	36±1.5
IEE223	L_1	5.5	2.22±0.09	12.20±0.27	1.94	20±2	0.044	3.32±0.12	168±6.4	189±5.7	50.7±2.6	57±2.7
IEE272	L_1	8.0	2.43±0.13	12.01±0.26	1.84	15±2	0.045	3.50±0.13	214±15	239±7.3	61.2±4.8	68±3.3
IEE228	L_1	8.5	2.40±0.10	11.40±0.25	1.88	15±2	0.056	3.59±0.13	232±4.4	257±7.3	64.6±2.6	72±3.5
IEE232	S_1	9.5	2.55±0.10	13.80±0.30	2.01	25±2	0.052	3.35±0.16	270±12	305±18	80.6±5.3	91±7.0
IEE270	S_1	10.6	2.48±0.14	15.50±0.34	2.09	20±2	0.039	3.51±0.16	341±16	309±14	97.3±6.5	88±5.6
IEE268	S_1	11.5	2.72±0.15	13.45±0.30	2.07	20±2	0.054	3.48±0.16	354±11	372±16	102±5.8	107±6.7
IEE266	S_1	12.3	2.61±0.14	13.07±0.29	1.96	20±2	0.040	3.24±0.15	409±18	393±8	126±8.1	121±6.1
IEE421	L_8	52.9	2.62±0.13	13.00±0.29	1.83	23±2	0.034	3.08±0.12	—	2382±88	—	774±41
IEE422	L_8	53.1	2.46±0.11	13.30±0.29	1.83	25±2	0.041	3.04±0.12	—	2296±86	—	755±41
IEE424	S_8	53.8	2.50±0.11	14.00±0.31	1.90	25±2	0.034	3.08±0.12	—	2433±76	—	790±39
IEE425	S_8	54.3	2.67±0.13	13.80±0.32	1.83	25±2	0.040	3.06±0.12	—	2339±118	—	765±48

References

Aitken, M.J., 1985. Thermoluminescence Dating. Academic Press, London.

Aitken, M.J., 1998. An Introduction to Optical Dating. Oxford University Press, Oxford.

Aitken, M.J., Smith, B.W., 1988. Optical dating: recuperation after bleaching. Quaternary Science Reviews 7, 387–393.

An, Z.S., Kukla, G., Porter, S.C., Xiao, J.L., 1991. Magnetic susceptibility evidence of monsoon variation on the Loess Plateau of central China during the last 130,000 years. Quaternary Research 36, 29–36.

An, Z.S., Lu, Y.C., 1984. A climatostratigraphic subdivision of Late Pleistocene strata named by Malan Formation in North China. Chinese Science Bulletin 29, 1239–1242.

Bailey, R.M., 2004. Paper I—simulation of dose absorption in quartz over geological timescales and its implications for the precision and accuracy of optical dating. Radiation Measurements 38, 299–310.

Chawla, S., Rao, T.K.G., Singhvi, A.K., 1998. Quartz thermoluminescence: dose and dose-rate effects and their implications. Radiation Measurements 29, 53–63.

Chen, R., Leung, P.L., 2000. A model for dose-rate dependence of thermoluminescence intensity. Journal of Physics D 33, 846–850.

Chen, R., Leung, P.L., 2001. Nonlinear dose dependence and dose-rate dependence of optically stimulated luminescence and thermoluminescence. Radiation Measurements 33, 475–481.

Coe, R.S., Singer, B.S., Pringle, M.S., Zhao, X., 2004. Matyama-Brunhes reversal and Kamikatsura event on Maui: paleomagnetic directions, $^{40}Ar/^{39}Ar$ ages and implications. Earth and Planetary Science Letters 222, 667–684.

Forman, S.L., 1991. Late Pleistocene chronology of loess deposition near Luochuan, China. Quaternary Research 36, 19–28.

Frechen, M., 1999. Luminescence dating of loessic sediments from the Loess Plateau, China. Geologische Rundschau 87, 675–684.

Heller, F., Liu, T.S., 1982. Magnetostratigraphical dating of loess deposits in China. Nature 300, 431–433.

Huang, C.C., Pang, J.L., Zhao, J.P., 2000. Chinese loess and the evolution of the east Asian monsoon. Progress in Physical Geography 24, 75–96.

Huntley, D.J., Godfrey-Smith, D.I., Thewalt, M.L.W., 1985. Optical dating of sediments. Nature 313, 105–107.

Huntley, D.J., Prescott, J.R., 2001. Improved methodology and new thermoluminescence ages for the dune sequence in south-east South Australia. Quaternary Science Reviews 20, 687–699.

Liu, T.S., et al., 1985. Loess and the Environment. China Ocean Press, Beijing.

Lu, Y.C., Prescott, J.R., Robertson, G.B., Hutton, J.T., 1987. Thermoluminescence dating of the Malan loess at Zhaitang, China. Geology 15, 603–605.

Lu, Y.C., Wang, X.L., Wintle, A.G., Accepted. A new OSL chronology for dust accumulation in the last 130,000 years for the Chinese Loess Plateau. Quaternary Research.

Lu, Y.C., Zhang, J.Z., Xie, J., 1988. Thermoluminescence dating of loess and paleosols from the Lantian section, Shaanxi Province, China. Quaternary Science Reviews 7, 245–250.

Lu, Y.C., Zhao, H., Yin, G.M., Chen, J., Zhang, J.Z., 1999. Luminescence dating of loess–palaeosol sequences in the past about 100 ka in North China. Bulletin of the National Museum of Japanese History 81, 209–220.

Martinson, D.G., Pisias, N.G., Hays, J.D., et al., 1987. Age dating and the orbital theory of the ice ages: development of a high-resolution 0–300,000 year chronostratigraphy. Quaternary Research 27, 1–29.

Murray, A.S., Wintle, A.G., 2000. Luminescence dating of quartz using an improved single-aliquot regenerative-dose protocol. Radiation Measurements 32, 57–73.

Musson, F.M., Clarke, M.L., Wintle, A.G., 1994. Luminescence dating of loess from the Liujiapo section, central China. Quaternary Science Reviews 13, 407–410.

Rhodes, E.J., 1988. Methodological considerations in the optical dating of quartz. Quaternary Science Reviews 7, 395–400.

Smith, B.W., Aitken, M.J., Rhodes, E.J., Robinson, P.D., Geldard, D.M., 1986. Optical dating: methodological aspects. Radiation Protection Dosimetry 17, 229–233.

Smith, B.W., Rhodes, E.J., 1994. Charge movements in quartz and their relevance to optical dating. Radiation Measurements 23, 329–334.

Spooner, N.A., Prescott, J.R., Hutton, J.T., 1988. The effect of illumination wavelength on the bleaching of the thermoluminescence (TL) of quartz. Quaternary Science Reviews 7, 325–329.

Valladas, G., Ferriera, J., 1980. On the dose-rate dependence of thermoluminescence response in quartz. Nuclear Instruments and Methods 175, 216–218.

Wang, X.L., Lu, Y.C., Zhao, H., 2006. On the performances of the single-aliquot regenerative-dose (SAR) protocol for Chinese loess: fine quartz and polyminerals. Radiation Measurements 41, 1–8.

Wang, X.L., Wintle, A.G., Lu, Y.C., Accepted. Thermally transferred luminescence in fine-grained quartz from Chinese loess: basic observations. Radiation Measurements, doi:10.1016/j.radmeas.2006.01.001.

Watanuki, T., Murray, A.S., Tsukamoto, S., 2005. Quartz and polymineral luminescence dating of Japanese loess over the last 0.6 Ma: comparison with an independent chronology. Earth and Planetary Science Letters 240, 774–789.

Zhou, L.P., Dodonov, A.E., Shackleton, N.J., 1995. Thermoluminescence dating of the Orkutsay loess section in the Tashkent region, Uzbekistan, Central Asia. Quaternary Science Reviews 14, 721–730.